4. OTHER ANALYSES

4.1 Pit 9 Overburden Contamination

The OU 7-10 Staged Interim Action Project plan called for excavation and retrieval of a small volume of Pit 9 waste. The first planned excavation step involves removal of overburden soil, which is estimated by Lange to extend to depths of 3–6 ft (Lange 1999). Lange presents evidence that Pit 9 overburden soils in this depth range may contain localized low-level alpha contamination from ^{241}Am and ^{239}Pu; however, the Lange sampling data provide no information on possible overburden contamination within the specific area proposed for the planned excavation and retrieval (Lange 1999). This report summarizes information obtained from downhole geophysical logging data that relates to overburden contamination at the proposed excavation site.

The limited Pit 9 retrieval is planned for the area surrounding Probe Hole P9-20. Probe Hole P9-20 and surrounding probe holes (P9-02, P9-03, P9-04, P9-05, P9-08, P9-09, P9-10, P9-11, P9-14, P9-19, and P9-20-01–P9-20-06) were logged using downhole nuclear logging tools with capabilities to detect gamma-emitting radionuclides including ^{239}Pu, ^{241}Am, ^{237}Np, ^{235}U, ^{238}U, ^{137}Cs, and ^{60}Co. Other logging tools were used to detect chlorine (possibly associated with chlorinated solvents) and to provide information about the soil/waste medium surrounding the probe holes, such as soil moisture and amounts of common soil forming elements.

4.1.1 Overburden and Waste Zone Boundary

Table 4-1 gives a summary of the interpreted depth of overburden soils in the excavation area based on geophysical logging data. Depths were interpreted using changes in Si/Ca and soil-moisture levels as the primary indicators of the soil-waste transition. Si/Ca concentrations and soil moisture are found to generally decrease within the 3–6-ft depth range, accompanied by a corresponding increase in gamma-ray flux from radionuclide contamination sources. The Table 4-1 depth estimates show that overburden soil depth in the excavation area is consistent with Lange's estimates for the overall Pit 9 area (Lange 1999).

4.1.2 Results of Type A Logging in The Overburden

Spectral gamma-ray logging data were used as the basis for identifying possible radionuclide contamination in overburden soils. The logging subcontractor used an automated peak analysis program that measured gamma-ray peak heights for contaminants of interest and estimated statistical uncertainty. For the current analysis, these data were first edited to eliminate measurements where uncertainty exceeded ± 30%. The 30% threshold was suggested by the logging subcontractor as an approximate lower confidence limit for individual measurements. The data were then compiled to show all indications for ^{239}Pu, ^{241}Am, ^{237}Np, ^{235}U, ^{238}U, ^{137}Cs, ^{60}Co, and chlorine within the upper 5 ft for the probe holes of interest. No detections were found for ^{235}U, ^{238}U, ^{137}Cs, and ^{60}Co. Tables 4-2–4-5 show results for ^{239}Pu, ^{241}Am, ^{237}Np, and chlorine.

The logging data show that radionuclide contamination occurs within the upper 5-ft soil layer but is confined (with two exceptions) to depths at or below 3.5 ft. Furthermore, the localized shallow contamination areas are continuous with contamination zones that reach their maximum apparent concentrations below 5 ft (P9-20 cluster and P9-03). Note that gamma radiation can penetrate through several inches of soil so that the point where the contamination actually begins is probably slightly deeper than the point where the logging tool first detects it. Taken together, these observations suggest that the majority of radionuclide detections above 5 ft are the result of a locally thin overburden, possibly combined with a small amount of radionuclide migration upward from the waste zone into the lower overburden soils.

Table 4-1. Approximate top of waste zone based on Type A logging data in Pit 9.

Well ID	Top of Waste (ft)
P9-02	5.0
P9-03	5.0
P9-04	6.0
P9-05	6.0
P9-08	5.5
P9-09	4.5
P9-10	5.5
P9-11	6.0
P9-14	3.5
P9-19	5.0
P9-20	4.5
P9-20-01	4.5
P9-20-02	4.5
P9-20-03	No estimate
P9-20-04	5.5
P9-20-05	4.5
P9-20-06	4.5

The noted exceptions to the general conditions are one indication of ^{239}Pu (11 nCi/g at 3 ft in P9-20-02) and one indication of ^{241}Am (22 nCi/g at 1 ft in P9-20-03). These measurements had high uncertainties (29–30%). The spectra associated with these measurements were examined and showed the presence of contamination to be doubtful in both cases. It is suspected that the indicated levels of contamination in these two cases are below the detection limit for the count times employed. Chlorine indications for the 0–5-ft range may be described with the same general observations as for the radionuclides (Table 4-5).

In summary, the logging data show the overburden in the vicinity of the planned excavation to be clean, at least to the level of detection allowed by the logging tools and count times employed; however, the overburden itself may be as thin as 3.5–4 ft in some places.

4.1.3 Limitations of Type A Logging Methods

Table 4-6 shows the logging subcontractor estimated nondetect limits for the radionuclides examined in this study. The estimates are based on statistical evaluation of background gamma-ray flux, against which anomalous gamma-ray peaks must be discerned. Careful examination of actual spectra for several low-level contamination cases supports these theoretical detection limit estimates. As a consequence, the "cleanness" of overburden soils cannot be unambiguously demonstrated beyond about 30 nCi/g for ^{241}Am and ^{239}Pu. Lower detection limits could be obtained by relogging the probes of interest using longer count times.

Table 4-2. Occurrences of ^{239}Pu (nCi/g equivalent) in the Pit 9 overburden based on spectral gamma-ray logging of Type A probes.

239Pu (depth)	P9-02	P9-03	P9-04	P9-05	P9-08	P9-09	P9-10	P9-11	P9-14	P9-19	P9-20	P9-20-01	P9-20-02	P9-20-03	P9-20-04	P9-20-05	P9-20-06
0.5	ND	ND	ND	ND	ND	ND	ND	ND	ND	ND	ND	ND	ND	ND	ND	ND	ND
1	ND	ND	ND	ND	ND	ND	ND	ND	ND	ND	ND	ND	ND	ND	ND	ND	ND
1.5	ND	ND	ND	ND	ND	ND	ND	ND	ND	ND	ND	ND	ND	ND	ND	ND	ND
2	ND	ND	ND	ND	ND	ND	ND	ND	ND	ND	ND	ND	ND	ND	ND	ND	ND
2.5	ND	ND	ND	ND	ND	ND	ND	ND	ND	ND	ND	ND	ND	ND	ND	ND	ND
3	ND	ND	ND	ND	ND	ND	ND	ND	ND	ND	ND	ND	11	ND	ND	ND	ND
3.5	ND	ND	ND	ND	ND	ND	ND	ND	ND	ND	ND	ND	170	ND	ND	ND	22
4	ND	ND	ND	ND	ND	ND	ND	ND	ND	ND	194	309	422	ND	ND	ND	390
4.5	ND	ND	ND	ND	ND	ND	ND	ND	ND	ND	2,273	1,148	994	170	ND	827	3,366
5	ND	65	ND	ND	ND	ND	ND	ND	ND	ND	23,920	3,516	2,104	1,755	ND	2,907	11,253

ND = nondetect

Table 4-3. Occurrences of ^{241}Am (nCi/g equivalent) in the Pit 9 overburden based on spectral gamma-ray logging of Type A probes.

241Am (depth)	P9-02	P9-03	P9-04	P9-05	P9-08	P9-09	P9-10	P9-11	P9-14	P9-19	P9-20	P9-20-01	P9-20-02	P9-20-03	P9-20-04	P9-20-05	P9-20-06
0.5	ND	ND	ND	ND	ND	ND	ND	ND	ND	ND	ND	ND	ND	ND	ND	ND	ND
1	ND	ND	ND	ND	ND	ND	ND	ND	ND	ND	ND	ND	ND	22	ND	ND	ND
1.5	ND	ND	ND	ND	ND	ND	ND	ND	ND	ND	ND	ND	ND	ND	ND	ND	ND
2	ND	ND	ND	ND	ND	ND	ND	ND	ND	ND	ND	ND	ND	ND	ND	ND	ND
2.5	ND	ND	ND	ND	ND	ND	ND	ND	ND	ND	ND	ND	ND	ND	ND	ND	ND
3	ND	ND	ND	ND	ND	ND	ND	ND	ND	ND	ND	ND	ND	ND	ND	ND	ND
3.5	ND	ND	ND	ND	ND	ND	ND	ND	ND	ND	ND	ND	ND	ND	ND	ND	ND
4	ND	ND	ND	ND	ND	ND	ND	ND	ND	ND	ND	81	69	19	ND	ND	42
4.5	ND	ND	ND	ND	ND	ND	ND	ND	ND	ND	349	204	160	32	ND	ND	488
5	ND	ND	ND	ND	ND	ND	ND	ND	ND	ND	2,830	570	528	296	ND	300	1,332

ND = nondetect

Table 4-4. Occurrences of ^{237}Np (pCi/g equivalent) in the Pit 9 overburden based on spectral gamma-ray logging of Type A probes.

^{237}Np (depth)	P9-02	P9-03	P9-04	P9-05	P9-08	P9-09	P9-10	P9-11	P9-14	P9-19	P9-20	P9-20-01	P9-20-02	P9-20-03	P9-20-04	P9-20-05	P9-20-06
0.5	ND	ND	ND	ND	ND	ND	ND	ND	ND	ND	ND	ND	ND	ND	ND	ND	ND
1	ND	ND	ND	ND	ND	ND	ND	ND	ND	ND	ND	ND	ND	ND	ND	ND	ND
1.5	ND	ND	ND	ND	ND	ND	ND	ND	ND	ND	ND	ND	ND	ND	ND	ND	ND
2	ND	ND	ND	ND	ND	ND	ND	ND	ND	ND	ND	ND	ND	ND	ND	ND	ND
2.5	ND	ND	ND	ND	ND	ND	ND	ND	ND	ND	ND	ND	ND	ND	ND	ND	ND
3	ND	ND	ND	ND	ND	ND	ND	ND	ND	ND	ND	ND	ND	ND	ND	ND	ND
3.5	ND	ND	ND	ND	ND	ND	ND	ND	ND	ND	ND	ND	ND	ND	ND	ND	ND
4	ND	ND	ND	ND	ND	ND	ND	ND	ND	ND	ND	ND	ND	ND	ND	ND	ND
4.5	ND	ND	ND	ND	ND	ND	ND	ND	ND	ND	ND	ND	ND	ND	ND	ND	9.4
5	ND	ND	ND	ND	ND	ND	ND	ND	ND	ND	ND	8.8	ND	3.1	ND	8.4	31.4

a. Values given for ^{233}Pa, daughter of ^{237}Np

ND = nondetect

Table 4-5. Chlorine occurrences (counts/sec) in the Pit 9 overburden based on neutron activation logging of Type A probes.

Chlorine (depth)	P9-02	P9-03	P9-04	P9-05	P9-08	P9-09	P9-10	P9-11	P9-14	P9-19	P9-20	P9-20-01	P9-20-02	P9-20-03	P9-20-04	P9-20-05	P9-20-06
0.5	ND	ND	ND	ND	ND	ND	ND	ND	ND	ND	ND	ND	ND	ND	ND	ND	ND
1	ND	ND	ND	ND	ND	ND	ND	ND	ND	ND	ND	ND	ND	ND	ND	ND	ND
1.5	ND	ND	ND	ND	ND	ND	ND	ND	ND	ND	0.3	ND	ND	ND	ND	ND	ND
2	ND	ND	ND	ND	ND	ND	ND	ND	ND	ND	ND	ND	ND	ND	ND	ND	ND
2.5	ND	ND	0.7	ND	ND	ND	ND	ND	ND	ND	ND	ND	ND	ND	ND	ND	ND
3	ND	ND	ND	ND	ND	ND	ND	ND	ND	ND	ND	ND	ND	ND	ND	ND	ND
3.5	ND	ND	ND	ND	ND	ND	ND	ND	ND	ND	ND	ND	ND	ND	ND	ND	ND
4	ND	ND	ND	ND	ND	ND	ND	ND	ND	ND	ND	ND	ND	ND	ND	ND	0.3
4.5	ND	ND	ND	ND	ND	ND	ND	ND	ND	ND	ND	ND	ND	ND	0.3	ND	4.4
5	ND	ND	ND	ND	ND	ND	ND	ND	0.7	0.9	0.9	1.9	ND	ND	ND	ND	12.4

ND = nondetect

Table 4-6. Theoretical detection limits for selected radionuclides based on logging data.

Radionuclide	Overburden Nondetect Limit[a]
^{235}U	1.8 pCi/g
^{233}Pa	1.7 pCi/g
^{239}Pu	27.2 nCi/g
^{241}Am	33.9 pCi/g
^{137}Cs	0.3 pCi/g

a. GTS Duratek defines a radionuclide's nondetect limit as the maximum concentration of the radionuclide that can be present in an otherwise clean environment without producing a statistically significant photo peak in the gamma-ray spectra.

4.1.4 Overburden Compaction

Drilling resistance was encountered at about 3.5–5 ft within many of the Pit 9 probes. In fact, the drilling probe tip had to be modified before this resistive zone could be penetrated in some cases. Logging data were reviewed to determine if the source of the resistance could be discovered. The resistive zone generally corresponds with the top of the waste zone where logging data show large changes in moisture, elemental composition, and radionuclide concentration. A unique explanation for the drilling resistance could not be isolated from other effects.

4.2 Soil Cover Thickness Estimates

Soil cover for pits and trenches at the SDA was estimated by Barnes based on records maintained by operations personnel beginning with pit and trench closure (Barnes 1989). Barnes's estimates are summarized in Table 4-7 (Barnes 1989).

4.3 Soil Cover Based on Type A Logging Data

Type A downhole logging data provide an alternative basis for estimating the thickness of soil cover above waste. One hundred thirty-seven Type A probes were installed in Pits 4, 5, 9, and 10 as shown in Table 4-8.

Physical and chemical changes in the character of the soil medium occur at the transition from soil to waste. These changes are often manifested in the logging tool response observed in passive gamma-ray, activated gamma-ray (n-gamma), and neutron-neutron moisture logs. The most common manifestations are a reduction in the n-gamma silicon and calcium response and changes in the apparent neutron-neutron water content, but other signatures are possible as listed in Table 4-9. On this principle, the transition from soil to waste was interpreted for 127 Type A logs, providing independent estimates of the soil cover depth. The remaining 10 Type A logs showed no transition indicating that the logs did not penetrate any significant waste material.

Table 4-10 gives the interpreted soil cover depths for each probe. Table 4-11 gives the soil cover estimates for each pit and shows a comparison with the soil cover depths estimated by Barnes. In general, the soil depths as estimated by the two independent methods are in agreement.

Table 4-7. Estimates of Subsurface Disposal Area soil cover thickness in feet based on operations records.

Disposal Site	Initial Thickness	Additions 1975–1979	Additions 1985–1987	Total Thickness	Proposed Addition
Pit 1	1.5-2.0	1.5-2.0	0.0	3.0-4.0	0-1.0
Pit 2	2.0-3.0	1.5-2.0	0.0	3.5-5.0	0-1.0
Pit 3	2.0-3.0	2.0-3.0	0.0	4.0-6.0	2.0-3.0
Pit 4	3.0	3.0-5.0	0-1.0	6.0-9.0	0-1.0
Pit 5	3.0	1.0-3.0	0-1.0	4.0-7.0	0-1.0
Pit 6	3.0	3.0-5.0	0-2.0	6.0-9.0	0-1.0
Pit 7	3.0	0.0	0-1.0	3.0-4.0	0-1.0
Pit 8	3.0	0.0	1.0-3.0	4.0-6.0	0-1.0
Pit 9	3.0	2.0-3.0	0-1.0	5.0-7.0	0-1.0
Pit 10	3.0	3.0-5.0	0.0	6.0-8.0	0-1.0
Pit 11	3.0	0.0	2.0-4.0	5.0-7.0	0-1.0
Pit 12	3.0	0.0	3.0-5.0	6.0-8.0	0-1.0
Pit 13	3.0	0.0	1.0-3.0	4.0-6.0	0-1.0
Pit 14-16	3.0	0.0	0.0	3.0	0-1.0
Trenches	0.0	0.0	0.0	0.0	0.0
1, 5, 7, 9	1.5-2.0	1.0-3.0	0.0	2.5-5.0	0-2.0
2, 3, 4, 6, 8, 10, 11, 13, 15	1.5-2.0	0.0	0.5-4.0	2.0-6.0	0-1.0
12, 14	1.5-2.0	0.0	0-1.0	1.5-3.0	0-1.0
16, 19, 23, 26, 28, 31, 34, 36	2.0-3.0	0.0	0.5-3.0	2.5-6.0	0-1.0
17, 58	2.0-3.0	0.0	1.0-4.0	3.0-7.0	0-1.0
18, 38	2.0-3.0	0.0	0-1.0	2.0-4.0	0-1.0
20, 25, 27, 30, 33, 35, 37, 39	2.0-3.0	0.0	1.0-2.0	3.0-5.0	0-1.0
21, 22, 24, 29, 32	2.0-3.0	0.0	0.0	2.0-3.0	2.0-3.0
40, 42, 45, 47, 49, 51, 53, 55	3.0	0.0	0-2.0	3.0-5.0	0-1.0
41, 43, 46, 48, 50, 52, 54, 56, 57	3.0	0.0	0-1.0	3.0-4.0	0-1.0
Acid Pit	2.0-3.0	0.0	2.0-4.0	4.0-7.0	0-1.0
Pad A	3.0	0.0		0.0	0.0
Soil vault rows	3.0	0.0	0-1.0	3.0-4.0	0-1.0
Areas between waste	0.0	0.0	0-5.0	0-5.0	0-2.0

Table 4-8. Type A probe installation summary.

Pit	Number of Type A Probes
4	31
5	14
9	49
10	41
Total	137

Table 4-9. Logging methods used for soil cover thickness interpretation.

Logging method	Soil indicators
Passive spectral gamma ray	^{40}K, ^{232}Th
Activated spectral gamma ray	Silicon, calcium, hydrogen, iron
Neutron-neutron	Hydrogen, void space

Table 4-10. Estimated soil cover thickness for Type A probe holes based on logging data.

Pit	Well ID	Soil Cover (ft)	Pit	Well ID	Soil Cover (ft)
10	741-02	7.9	4	743-12	11.0
10	741-03	7.3	4	743-13	10.0
10	741-04	7.4	4	743-14	11.0
10	741-06	6.7	4	743-15	11.0
10	741-08	5.8	4	743-16	9.0
10	741-08-A	9.5	4	743-17	9.0
10	741-08-B	9.5	4	743-18	10.0
10	741-09	9.7	4	743-20	9.5
4	743-01	7.0	4	743-21	12.5
4	743-02	6.5	4	743-22	10.0
4	743-03	7.0	4	743-23	No waste
4	743-04	7.0	4	743-24	9.5
4	743-05	8.0	4	743-25	5.5
4	743-06	7.0	4	743-32	6.0
4	743-07	7.0	4	743-33	No waste
4	743-08	10.5	4	743-34	No waste
4	743-08-01	8.0	4	743-35	9.3
4	743-08-02	9.0	4	743-36	7.0
4	743-08-03	8.0	4	743-37	8.6
4	743-08-04	9.0	4	743-38	6.7
4	743-08-05	9.5	4	743-39	6.7
4	743-08-06	9.0	4	743-40	5.8
4	743-09	8.0	4	743-41	11.8
4	743-10	9.0	4	743-42	8.4
4	743-11	11.0	10	DU-01	4.7

Table 4-10. (continued).

Pit	Well ID	Soil Cover (ft)
10	DU-02	5.8
10	DU-03	5.3
10	DU-04	No waste
10	DU-05	5.9
10	DU-06	5.2
10	DU-07	5.6
10	DU-08	5.2
10	DU-08-A	4.5
10	DU-08-B	5.0
10	DU-09	5.3
10	DU-10	4.6
10	DU-10-A	7.0
10	DU-10-B	7.0
10	DU-11	4.9
10	DU-12	6.4
10	DU-13	6.3
10	DU-14	5.5
10	DU-14-A	7.0
10	DU-14-B	5.0
10	DU-15	5.8
10	DU-16	5.4
10	DU-17	6.0
5	P5-1-1	No waste
5	P5-1-2	No waste
5	P5-1-3	No waste
5	P5-1-4	4.5
5	P5-1-6	6.0
5	P5-1-7	4.5
5	P5-1-8	4.5
5	P5-4-1	6.5
5	P5-4-2	6.0
5	P5-4-3	4.5
5	P5-4-4	6.0
5	P5-4-5	5.0
5	P5-4-6	5.0
5	P5-4-7	5.5
9	P9-01	5.5
9	P9-02	5.5
9	P9-03	5.3
9	P9-04	6.0
9	P9-05	7.2
9	P9-06	7.0
9	P9-07	5.5
9	P9-08	7.0
9	P9-09	5.5
9	P9-10	6.0
9	P9-11	6.0
9	P9-12	5.5
9	P9-13	5.0
9	P9-14	5.5
9	P9-15	5.0
9	P9-16	5.0
9	P9-17	6.5
9	P9-18	5.5
9	P9-19	5.5
9	P9-20	5.0
9	P9-20-01	4.5
9	P9-20-02	5.0
9	P9-20-03	6.0
9	P9-20-04	5.5
9	P9-20-05	5.0
9	P9-20-06	5.0
9	P9-21A	7.5
9	P9-22	5.5
9	P9-23	6.0
9	P9-24A	5.0
9	P9-25A	7.5
9	P9-26A	7.5
9	P9-27	5.0
9	P9-28A	No waste
9	P9-FI-01	7.5
9	P9-FI-02	6.0
9	P9-FI-03	7.0
9	P9-FI-04	6.5
9	P9-FI-05	9.5
9	P9-FI-06	6.5
9	P9-FI-07	5.5
9	P9-FI-08	9.5
9	P9-GR-01	5.5
9	P9-GR-02	4.0
9	P9-GR-03	5.0
9	P9-GR-04	7.0
9	P9-GR-05	4.5
9	P9-GR-06	5.0
9	P9-GR-07	4.5

Table 4-11. Minimum, maximum, and average soil cover thickness for Pits 4, 5, 9,and 10 based on Type A logging data.

Pit	Number	Minimum (ft)	Maximum (ft)	Average (ft)	Barnes estimate (ft)
Pit 4	30	4.5	9.7	6.2	6–9
Pit 5	11	4.5	6.5	5.3	4–7
Pit 9	48	4.0	9.5	5.9	5–7
Pit 10	38	5.5	12.5	8.7	6–8
Total	127	4.0	12.5	6.8	NA

4.3.1 Soil Cover Estimates Based on Surface Geophysics Data

Harding Lawson Associates conducted a high resolution geophysical survey of Pits 4, 6, and 10 in 1999. Geophysical data included vertical gradient magnetic data and induction EM data. In their report, the subcontractor includes a summary of depth estimates based on the magnetic and EM data (see Appendix A). These depth estimates are based on empirical methods and apply only to metallic objects. The subcontractor depth analysis results are reproduced in Table 4-12 and give another independent estimate of soil cover at the SDA.

Table 4-12. Minimum, maximum, and average soil cover thickness for Pits 4, 5, 9, and 10 based on surface geophysics data.

Pit	Method	Number	Minimum (ft)	Maximum (ft)	Average (ft)	Barnes estimate (ft)
Pit 4	Magnetics	21	2.8	14.2	6.7	6–9
	EM	22	2.8	8.9	6.9	
Pit 6	Magnetics	7	4.5	12.8	7.2	4–7
	EM	4	6.8	10.5	8.3	
Pit- 10	Magnetics	33	3.6	17	7.7	6–8
	EM	21	2.3	7.5	5.8	

EM = electromagnetics

4.4 Waste Zone Thickness

Type A downhole logging data provide a basis for estimating the top and bottom of the waste zone within the probed areas of Pits 4, 5, 9, and 10.

4.4.1 Principle

The upper and lower waste boundary interpretation is based on the principle that the waste zone contains less soil and greater void space than the overlying cap and underburden, although pockets of pure soil may certainly be scattered throughout the interior of the waste zone. On this principle, logging data were used to identify reductions in the amount of common soil components, especially silicon and

potassium, as well as changes in water content and void space as indicated by moisture log data. These reductions were interpreted to reflect the transition from pure soil to soil-waste mixtures. The shallowest transition was marked as the upper waste boundary and the deepest transition was marked as the lower waste boundary.

4.4.2 Method

Silicon, potassium, and moisture logs were the primary data sets used for interpreting waste boundaries, but thorium, calcium, hydrogen, and iron were also considered. Table 4-13 shows the logging methods utilized for the various soil indicators. For each well-grouping (i.e., 741, 743, and DU Study Areas), logging data were compiled into cross sections to accommodate recognition of trends between probes. A trendline representing the interpreted position of the soil-waste transition was constructed across each cross section. Interpreted boundaries were then compared against contamination indicators (gross gamma, gross neutrons, and chlorine) to assure consistency and to recognize noise sources.

Table 4-13. Logging methods used for waste boundary interpretation.

Logging method	Soil indicators
Passive spectral gamma ray	^{40}K, ^{232}Th
Activated spectral gamma ray	Silicon, calcium, hydrogen, iron
Neutron-neutron	Hydrogen, void space

Depth to basalt was assumed to correspond with the drilling total depth, which was measured by the drilling crew after probe installation. In cases where total depth was not measured, depth to basalt was estimated based on the maximum logging depth, which averaged 0.6 ft above total depth.

4.4.3 Results

Estimated depths to basalt, top of waste, and bottom of waste are compiled in Table 4-14. In some cases, no lower waste boundary was recognized. In these cases, the boundary was assumed to lie below the maximum logged depth, and Table 4-14 gives maximum logged depth as the minimum depth of this boundary.

Table 4-14. Waste boundary depths and depth to basalt based on logging data interpretation.

Well ID	Top of Waste	Bottom of Waste	Maximum Logged Depth	Drilling Total Depth	Depth to Basalt
741-02	8.5	>17.5	17.5	18.1	18.1
741-03	8.0	>18.5	18.7	20.3	20.3
741-04	8.5	14.5	23.7	24.3	24.3
741-06	9.0	>17.0	17.4	18.0	18.0
741-08	7.0	20.0	21.3	22.3	22.3
741-08-A	8.5	>20.0	20.4	20.8	20.8
741-08-B	8.0	18.0	21.4	21.8	21.8
741-09	8.0	>13.5	13.8	14.3	14.3

Table 4-14. (continued).

Well ID	Top of Waste	Bottom of Waste	Maximum Logged Depth	Drilling Total Depth	Depth to Basalt
743-01	5.0	13.5	15.5	17.2	17.2
743-02	5.0	14.5	19.4	20.7	20.7
743-03	5.5	15.0	19.1	19.5	19.5
743-04	6.0	16.5	24.6	25.5	25.5
743-05	6.5	23.5	26.3	27.0	27.0
743-06	5.5	25.0	25.8	26.2	26.2
743-07	7.0	>24.5	24.7	25.3	25.3
743-08	9.0	>24.5	24.9	25.3	25.3
743-08-01	8.0	>25.0	25.2	25.6	25.6
743-08-02	8.5	>25.5	25.5	25.0	25.0
743-08-03	8.0	24.5	25.0	26.3	26.3
743-08-04	9.0	>24.5	24.5	25.1	25.1
743-08-05	9.0	>23.5	23.7	25.0	25.0
743-08-06	9.0	>24.5	24.5	25.1	25.1
743-09	7.5	>23.5	23.8	24.3	24.3
743-10	8.0	>25.0	25.4	25.8	25.8
743-11	9.0	>24.5	24.9	25.5	25.5
743-12	9.0	>24.0	24.4	25.0	25.0
743-13	7.5	>25.0	25.0	25.6	25.6
743-14	10.5	>22.0	22.4	23.0	23.0
743-15	11.0	>21.0	21.4	21.9	21.9
743-16	9.0	>14.5	14.9	16.2	16.2
743-17	9.5	17.0	19.2	20.7	20.7
743-18	9.5	16.0	20.5	21.0	21.0
743-20	12.0	>15.5	15.7	16.3	16.3
743-21	12.0	>12.5	12.7	14.8	14.8
743-22	10.5	16.0	20.8	21.4	21.4
743-23	No Waste	No Waste	7.8	8.4	8.4
743-24	7.5	14.5	22.5	23.5	23.5
743-25	8.5	15.0	17.3	17.8	17.8
743-32	5.0	>12.0	12.0	12.1	12.1
743-33	No Waste	No Waste	11.4	12.1	12.1

Table 4-14. (continued).

Well ID	Top of Waste	Bottom of Waste	Maximum Logged Depth	Drilling Total Depth	Depth to Basalt
743-34	No Waste	No Waste	11.3	11.9	11.9
743-35	5.5	14.5	15.8	16.4	16.4
743-36	6.0	17.0	25.4	25.8	25.8
743-37	7.0	20.0	25.5	25.8	25.8
743-38	5.0	>14.5	14.9	15.5	15.5
743-39	5.0	15.5	23.3	19.8	19.8
743-40	5.0	15.0	19.8	18.4	18.4
743-41	4.0	15.5	22.1	21.5	21.5
743-42	6.0	15.5	21.9	22.2	22.2
DU-01	4.5	10.5	13.7	14.3	14.3
DU-02	5.5	10.0	12.0	14.8	14.8
DU-03	5.0	9.5	13.8	14.5	14.5
DU-04	No Waste	No Waste	13.4	14.0	14.0
DU-05	5.5	9.0	17.8	18.3	18.3
DU-06	5.5	10.5	17.7	18.5	18.5
DU-07	6.5	9.5	13.8	14.5	14.5
DU-08	4.5	17.0	17.7	18.7	18.7
DU-08-A	4.5	16.5	17.7	18.1	18.1
DU-08-B	5.0	16.0	18.6	17.6	17.6
DU-09	6.0	9.5	12.9	18.5	18.5
DU-10	4.0	9.5	16.8	17.3	17.3
DU-10-A	7.0	9.0	16.5	17.0	17.0
DU-10-B	6.5	10.0	16.8	17.2	17.2
DU-11	6.5	15.5	17.5	18.1	18.1
DU-12	6.0	13.5	17.8	18.3	18.3
DU-13	6.0	15.0	17.6	18.1	18.1
DU-14	5.0	>16.5	16.7	17.3	17.3
DU-14-A	6.0	>17.0	17.4	17.5	17.5
DU-14-B	6.0	16.0	17.0	17.6	17.6
DU-15	7.0	16.0	16.6	17.1	17.1
DU-16	5.5	>15.5	15.9	16.3	16.3
DU-17	5.5	18.5	19.7	20.2	20.2

Table 4-14. (continued).

Well ID	Top of Waste	Bottom of Waste	Maximum Logged Depth	Drilling Total Depth	Depth to Basalt
P5-1-1	6.0	>7.3	7.3	7.8	7.8
P5-1-2	6.5	>7.5	7.5	7.8	7.8
P5-1-3	No Waste	No Waste	8.5	9.1	9.1
P5-1-4	4.0	>8.0	8.0	8.5	8.5
P5-1-6	6.0	10.0	11.3	11.7	11.7
P5-1-7	3.5	10.0	15.0	16.0	16.0
P5-1-8	4.0	11.5	13.2	13.6	13.6
P5-4-1	6.5	16.0	16.2	16.5	16.5
P5-4-2	6.0	14.5	16.1	16.4	16.4
P5-4-3	4.5	13.5	15.9	16.3	16.3
P5-4-4	6.0	11.5	12.4	12.7	12.7
P5-4-5	5.0	10.0	10.0	10.5	10.5
P5-4-6	5.0	15.0	16.2	16.5	16.5
P5-4-7	5.5	13.0	13.8	14.1	14.1
P9-01	5.5	12.0	12.9	13.9	13.9
P9-02	5.5	11.0	14.4	15.5	15.5
P9-03	5.0	>10.5	10.6	11.5	11.5
P9-04	5.0	11.0	15.6	16.5	16.5
P9-05	6.5	11.5	15.9	16.9	16.9
P9-06	5.5	11.5	13.4	14.5	14.5
P9-07	5.5	11.0	14.9	15.8	15.8
P9-08	5.0	10.5	12.6	13.5	13.5
P9-09	4.0	>10.0	10.4	11.5	11.5
P9-10	5.0	>8.0	8.1	9.5	9.5
P9-11	5.5	10.5	14.1	15.0	15.0
P9-12	5.0	10.5	15.4	16.5	16.5
P9-13	4.5	10.5	14.9	15.8	15.8
P9-14	4.0	9.5	13.4	14.5	14.5
P9-15	3.5	8.5	12.4	13.5	13.5
P9-16	4.0	9.0	12.1	13.8	13.8
P9-17	6.0	9.5	13.9	14.8	14.8
P9-18	4.0	10.0	17.1	18.0	18.0

Table 4-14. (continued).

Well ID	Top of Waste	Bottom of Waste	Maximum Logged Depth	Drilling Total Depth	Depth to Basalt
P9-19	4.0	10.5	14.1	15.0	15.0
P9-20	4.0	10.5	11.9	12.3	12.3
P9-20-01	4.0	11.0	13.4	13.9	13.9
P9-20-02	3.5	9.5	12.2	11.6	11.6
P9-20-03	4.0	10.5	11.9	12.2	12.2
P9-20-04	4.5	10.5	12.3	12.6	12.6
P9-20-05	4.0	10.5	11.5	12.0	12.0
P9-20-06	4.0	10.5	11.9	12.3	12.3
P9-21A	7.5	11.5	12.6	13.3	13.3
P9-22	5.0	11.5	11.9	12.3	12.3
P9-23	6.0	>10.5	11.0	11.4	11.4
P9-24A	4.5	10.5	12.0	12.7	12.7
P9-25A	7.0	9.5	10.9	11.4	11.4
P9-26A	8.0	>10.5	10.8	11.3	11.3
P9-27	5.0	>10.9	10.9	11.3	11.3
P9-28A	No Waste	No Waste	9.5	10.1	10.1
P9-FI-01	7.5	>10.5	10.8	10.1	10.1
P9-FI-02	5.5	11.0	11.9	12.1	12.1
P9-FI-03	7.0	13.0	15.9	16.3	16.3
P9-FI-04	6.5	12.5	15.6	13.2	13.2
P9-FI-05	No Waste	No Waste	12.0	13.2	13.2
P9-FI-06	4.5	13.5	17.5	17.9	17.9
P9-FI-07	4.5	12.0	15.6	16.0	16.0
P9-FI-08	9.5	13.0	15.7	16.2	16.2
P9-GR-01	6.5	12.0	12.5	13.7	13.7
P9-GR-02	4.0	12.0	13.2	13.8	13.8
P9-GR-03	5.0	11.5	13.1	13.8	13.8
P9-GR-04	7.0	11.5	13.2	11.5	11.5
P9-GR-05	4.5	>10.5	10.8	11.5	11.5
P9-GR-06	5.5	>10.5	10.9	11.2	11.2
P9-GR-07	3.5	11.5	12.8	12.8	12.8

4.5 Well Screening Study

Per OU 7-13/14 Probing Project direction, the location of the proposed deep extraction, shallow extraction, and intermediate extraction wells and proposed shallow soil-vapor monitoring wells were evaluated using available surface geophysics data. Jason Casper provided the general location of the proposed wells by scaled drawings. The proposed locations for these wells are shown in Figure 4-1.

4.5.1 Method

Scaled drawings of the proposed well locations were used to determine starting coordinates for the new wells. These locations were compared against existing surface geophysical data for the SDA, which included vertical gradient magnetic data and electromagnetic induction data. Geophysical maps were examined to determine if any of the proposed well locations occurred within areas containing buried metal objects. Where conflicts were found, the proposed location was adjusted to an area interpreted to contain no metal objects. After adjustment, final coordinates were established for the wells and forwarded to the project field coordinator.

4.5.2 Results

Proposed Well IE-1 was located outside the SDA boundary. No geophysical data were available to screen this location. The location of SV-1 occurs within the Transuranic Storage Area facility and should be evaluated against existing Transuranic Storage Area infrastructure maps.

The remaining proposed well locations were screened using existing geophysical data. The proposed locations for the Series-6 wells occurred in an area having high resolution geophysics coverage, and were adjusted slightly to obtain greater clearance from buried metal objects (Figure 4-2). Series-3 wells were adjusted westward into an area having high-resolution geophysics coverage, and placed in locations free from buried metal objects (Figure 4-3). The proposed Series-4 and Series-5 wells were located in areas having only low-resolution geophysical data. The Series-4 well locations appear to be free of buried metallic materials over a wide area and are well clear of any known buried waste pits or trenches (Figure 4-4). The proposed Series-5 wells were located inside the historic boundary of Pit 12. Although it appeared that locations free from metallic waste could be found within Pit 12 (Figure 4-5), alternative locations were determined between Pits 11 and 12 (Figure 4-6).

After the initial well-location recommendations were made, it was found that the recommended location for Series-6 wells conflicted with a utility line on the ground surface between Pits 4 and 6. New locations were recommended as shown in Figure 4-7.

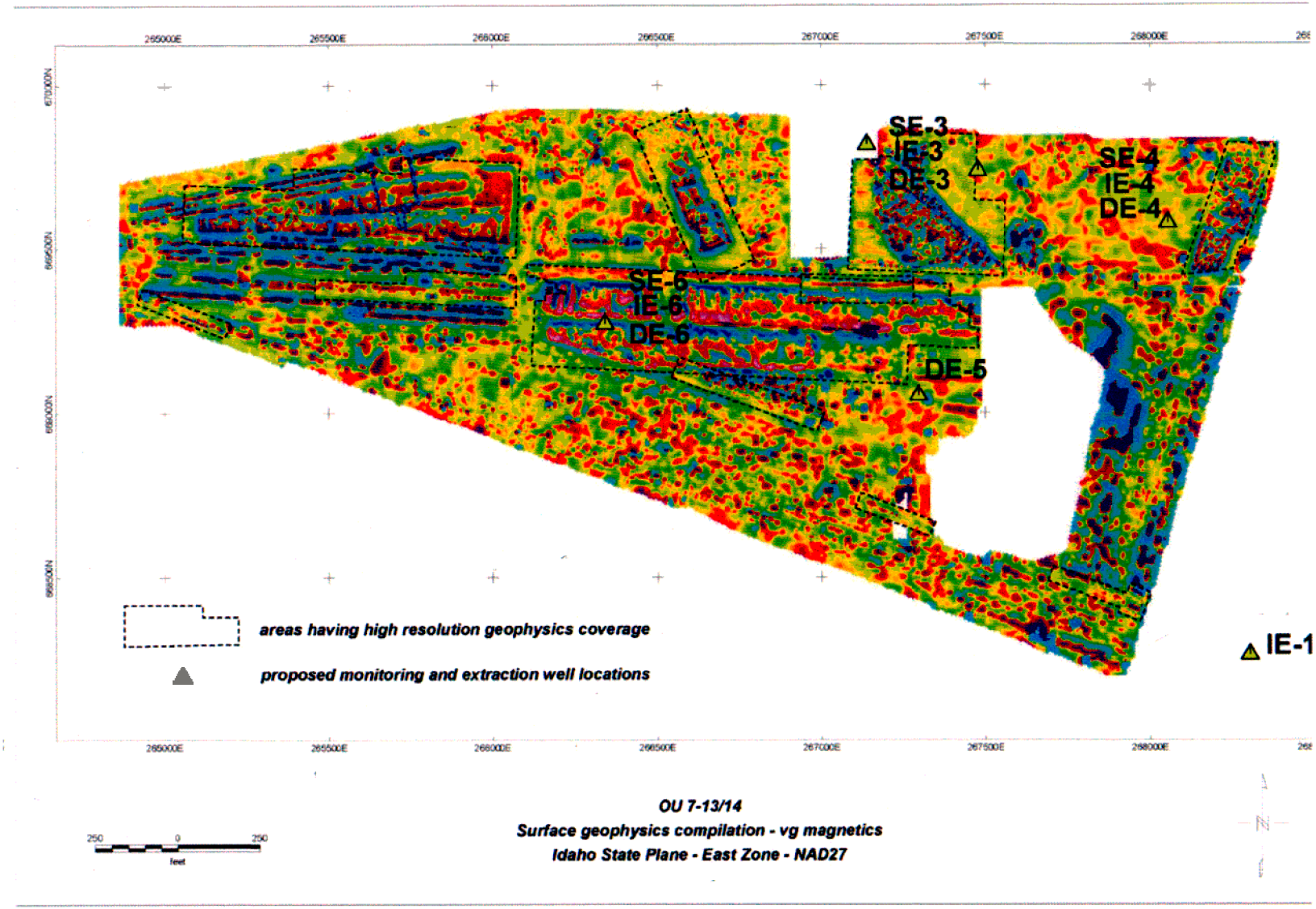

Figure 4-1. Original proposed location for new soil vapor monitoring and extraction wells at the Subsurface Disposal Area.

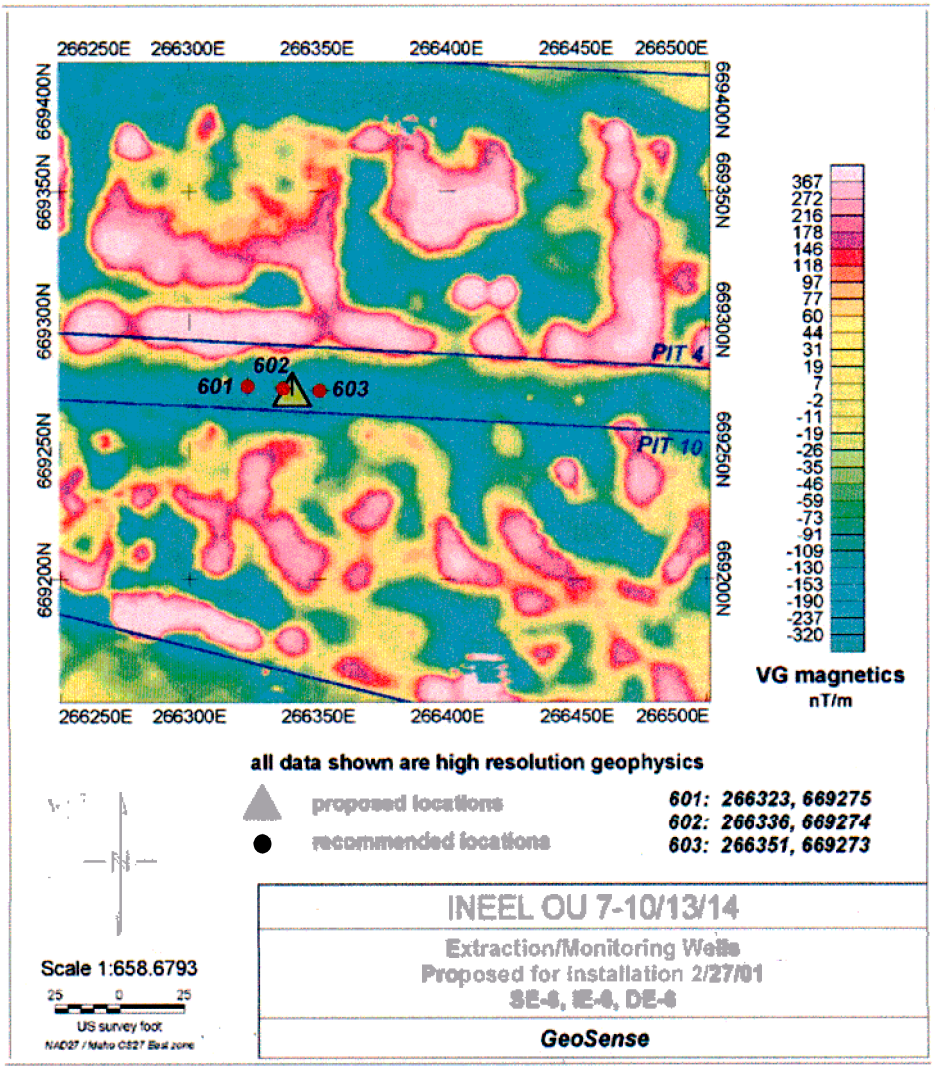

Figure 4-2. Proposed and recommended locations for Series-6 wells.

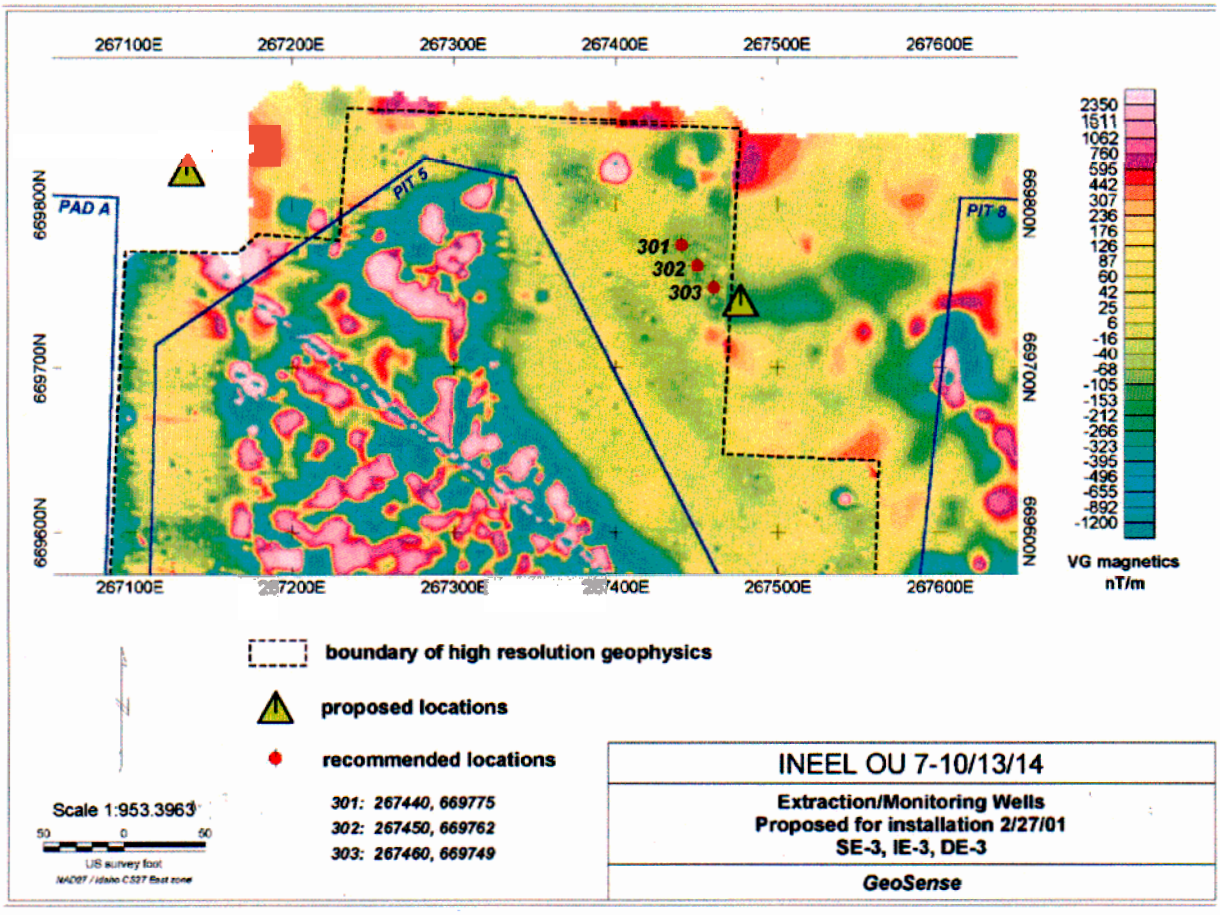

Figure 4-3. Proposed and recommended locations for Series-3 wells.

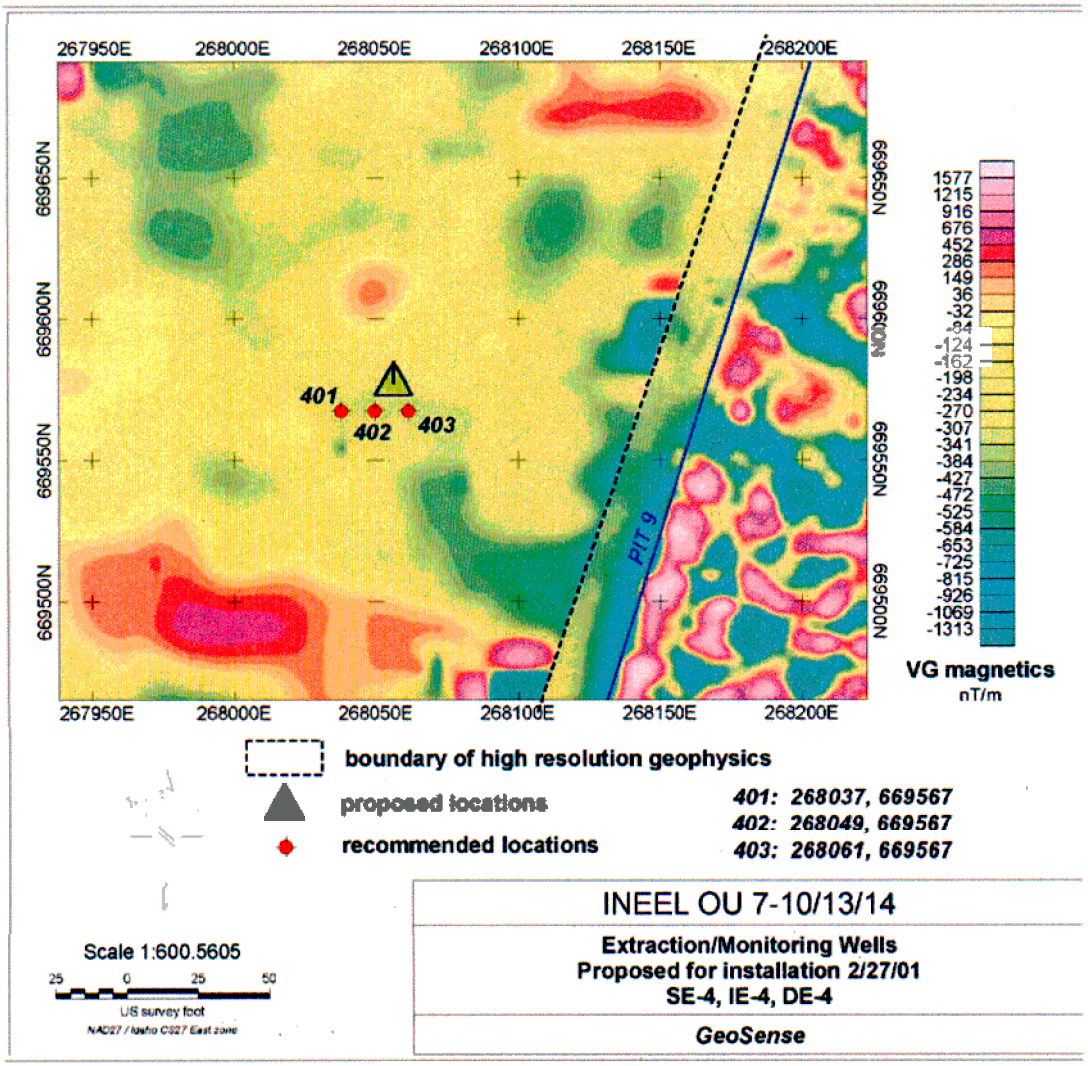

Figure 4-4. Proposed and recommended locations for Series-4 wells.

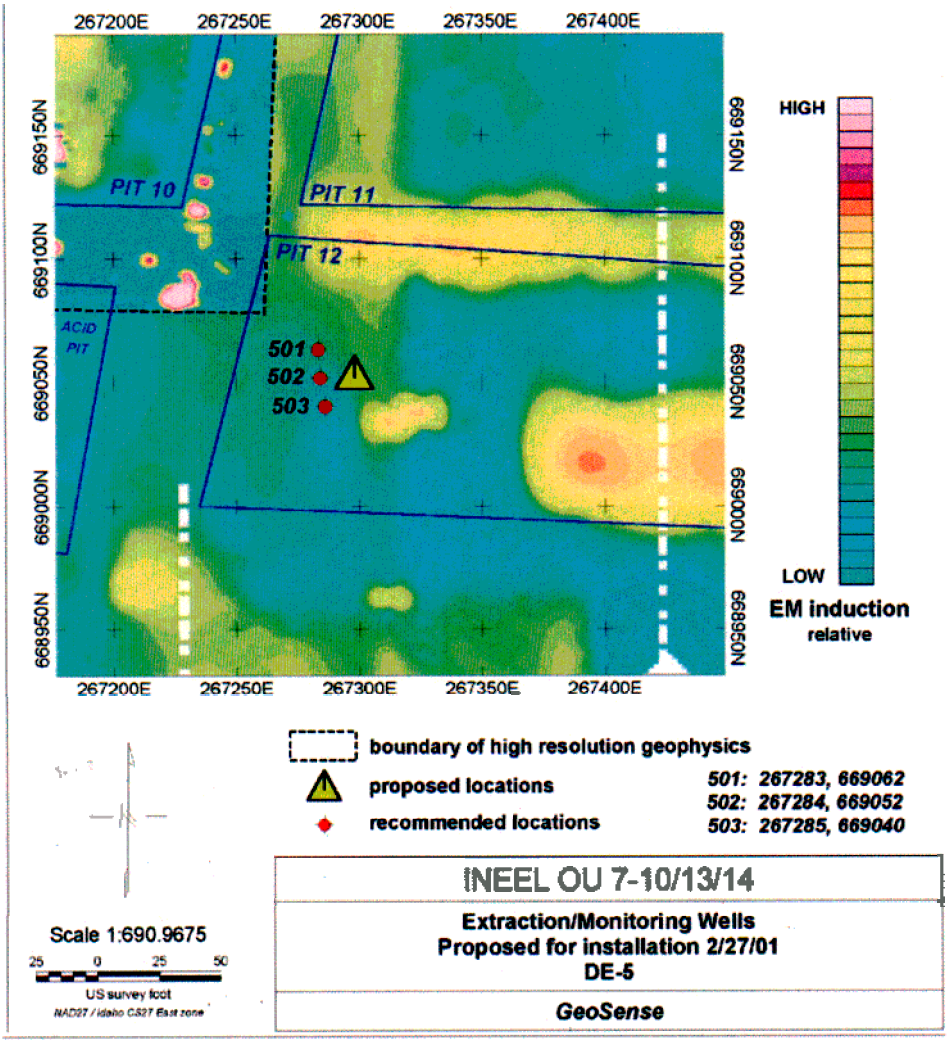

Figure 4-5. Proposed and recommended locations for Series-5 wells.

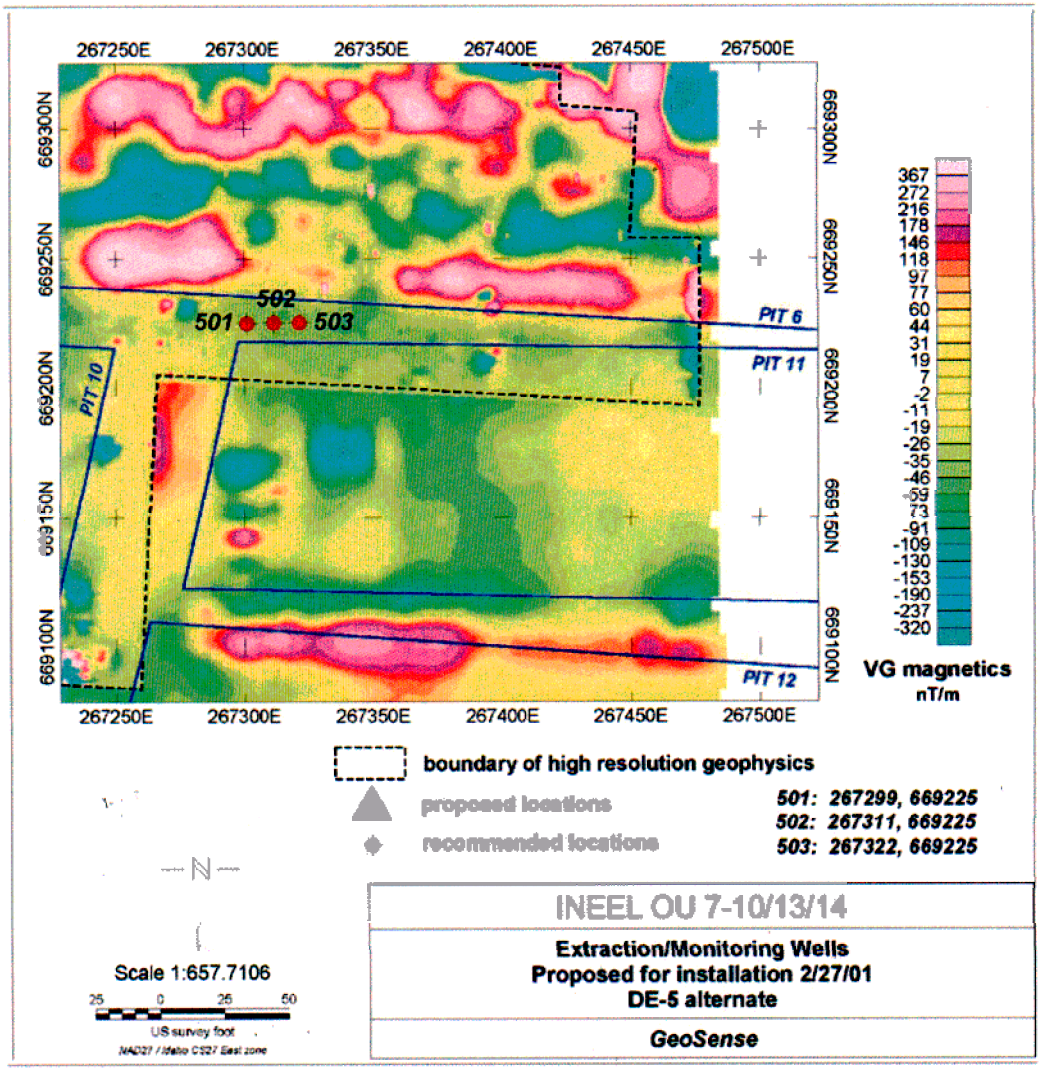

Figure 4-6. Alternative locations for Series-5 wells.

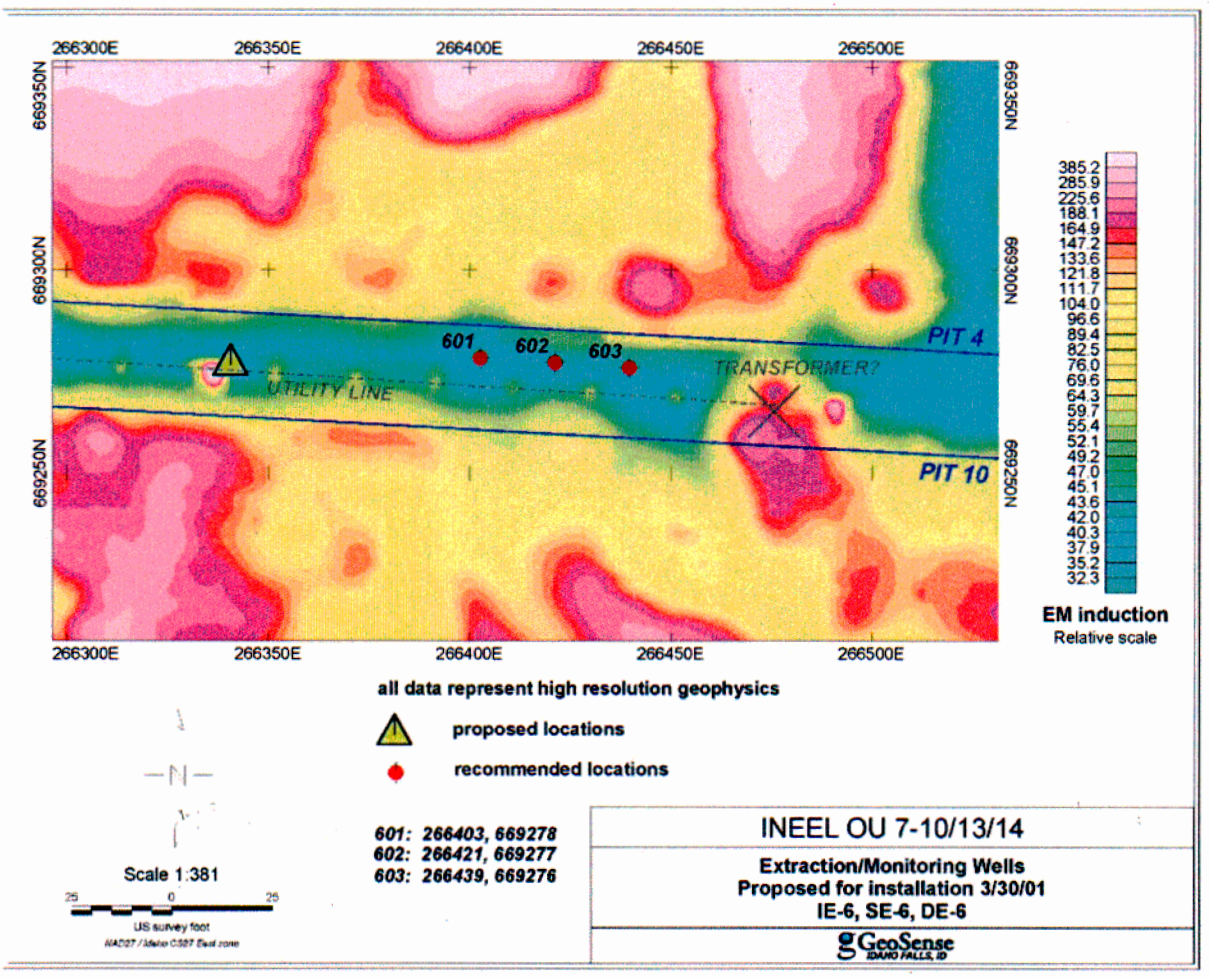

Figure 4-7. Alternative locations for Series-6 wells.

4.6 Plutonium, Americium, and Neptunium Enrichment Study

Type A logging measurements provide a basis for investigating radionuclide activity ratios (such as Pu and Am and Am and Np) on an SDA-wide basis. Out of 4,863 individual passive gamma-ray logging measurements, apparent Pu and Am ratios could be computed at 844 measurement points and Am and Np ratios could be computed at 469 points. Table 4-15 shows observed Pu and Am and Am and Np activity ratios based on these data. Histograms are shown in Figure 4-8. These observations are preliminary and are based on logging subcontractor data compilations, which assume uniform radionuclide distribution throughout the region surrounding the probe hole.

Table 4-15. Comparison of expected and observed Pu, Am, and Np activity ratios.

Ratio	Predominant Observed Activity Ratio	Number of Measurements
^{239}Pu:^{241}Am	7	844
^{241}Am:^{237}Np	32,000	469

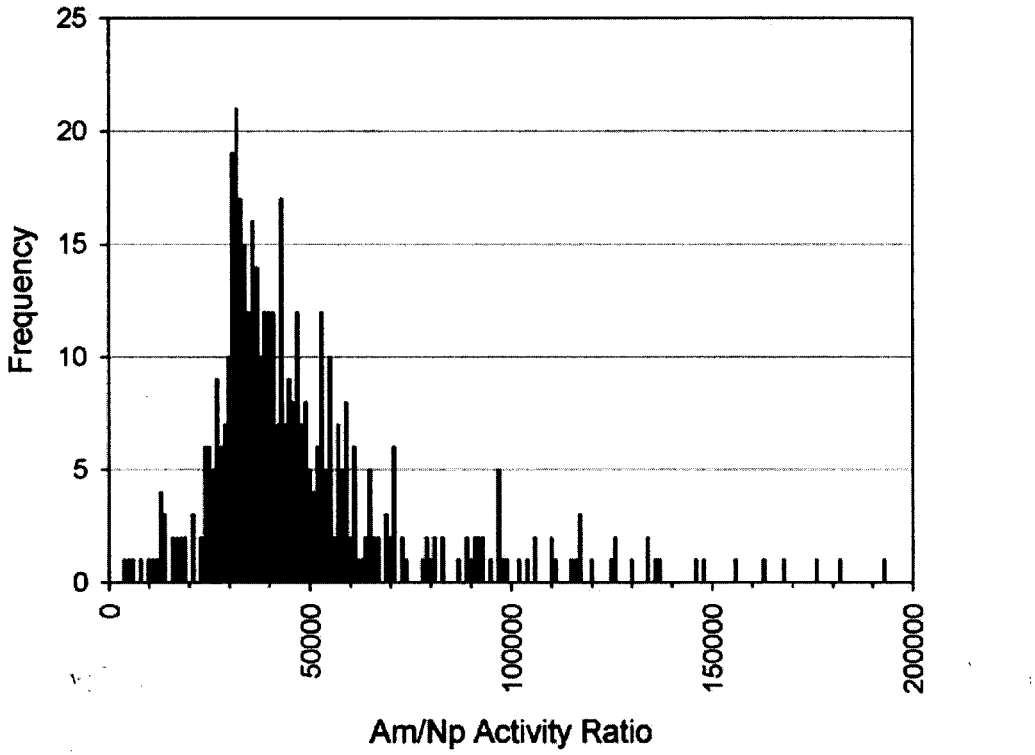

Figure 4-8. Histogram of Pu and Am activity ratios (upper) and Am and Np activity ratios (lower) compiled from all available Subsurface Disposal Area probe hole logging data.

4.7 Subsurface Disposal Area Soil Density

In support of the SDA probe hole logging program, it was necessary to determine an overall average soil density. This density was a factor in determining appropriate calibration and data reduction procedures for the logging data. Soil density data were compiled from previous reports by several authors (Borghese 1988; McElroy and Hubbel 1990; McElroy 1993; Shakofsky 1995). Figure 4-9 shows a histogram of the compiled density data.

4.8 P9-20 Plutonium Mass Estimate

One strategy for determining the Pu source mass near P9-20 takes advantage of the probe cluster geometry and azimuthal logging results. The method is based on three principles:

- Differential attenuation calculations can be used to estimate distance to the leading edge of the Pu mass distribution
- Azimuthal logs can be used to estimate the direction to the Pu center of mass
- Monte Carlo modeling can be used to determine a Pu mass distribution consistent with all constraints.

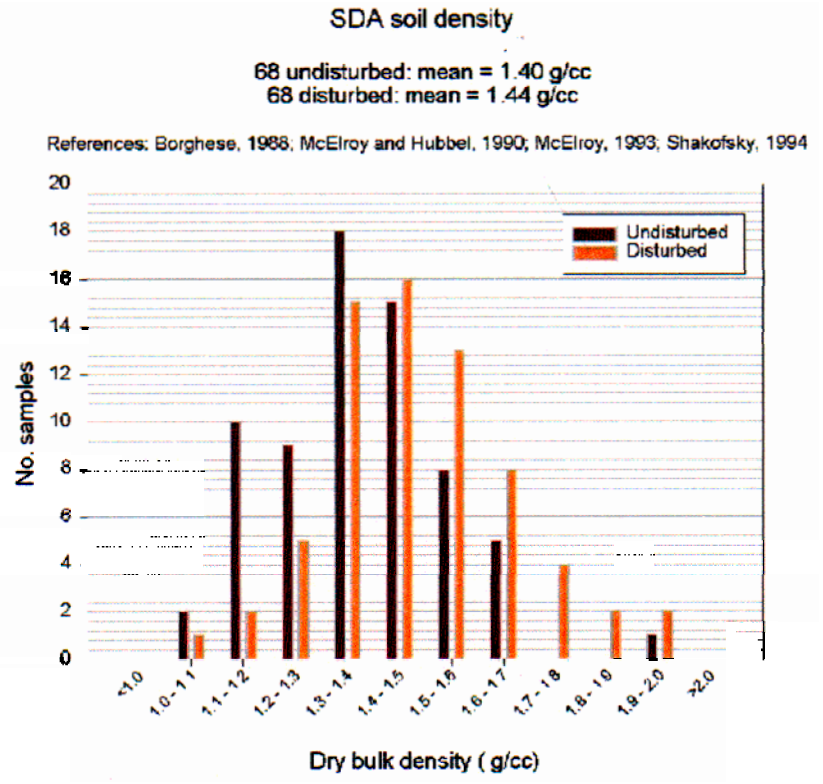

Figure 4-9. Histogram of Subsurface Disposal Area soil density data.

The first two principles are illustrated for a single probe in Figure 4-10. Note that this illustration shows the ambiguous nature of the single probe problem, owing to the fact that much of the Pu source volume can potentially occur outside the logging radius of investigation (90% attenuation limit).

By surrounding P9-20 with six additional probes on 1.5-foot centers, multiple distance-direction indicators may be generated for the source mass of interest. Some possible results are shown in Figure 4-11. For these cases, we show a "solution" that is consistent with the distance-direction indicators and with the further condition that the Pu distribution be uniform and continuous.

Figure 4-12 shows several alternative solutions without the uniform and continuous requirements. It is not known whether the logging data will distinguish between these alternative solutions since a small portion of the interprobe space occurs outside the volume of investigation of all the probes. This ambiguity creates the largest source of mass estimate error. The question is, how large could this error be?

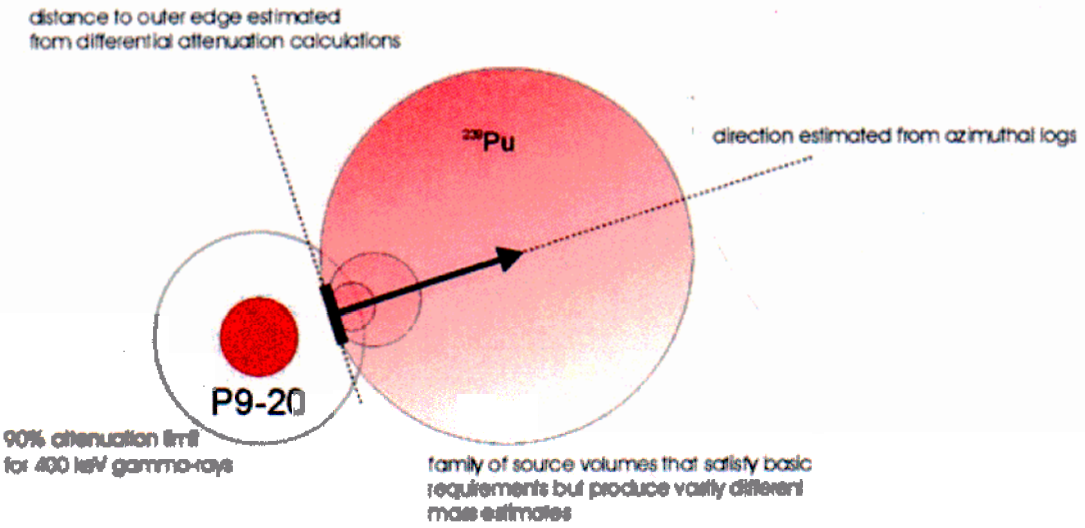

Figure 4-10. Use of differential attenuation and azimuthal logging to constrain source mass calculation.

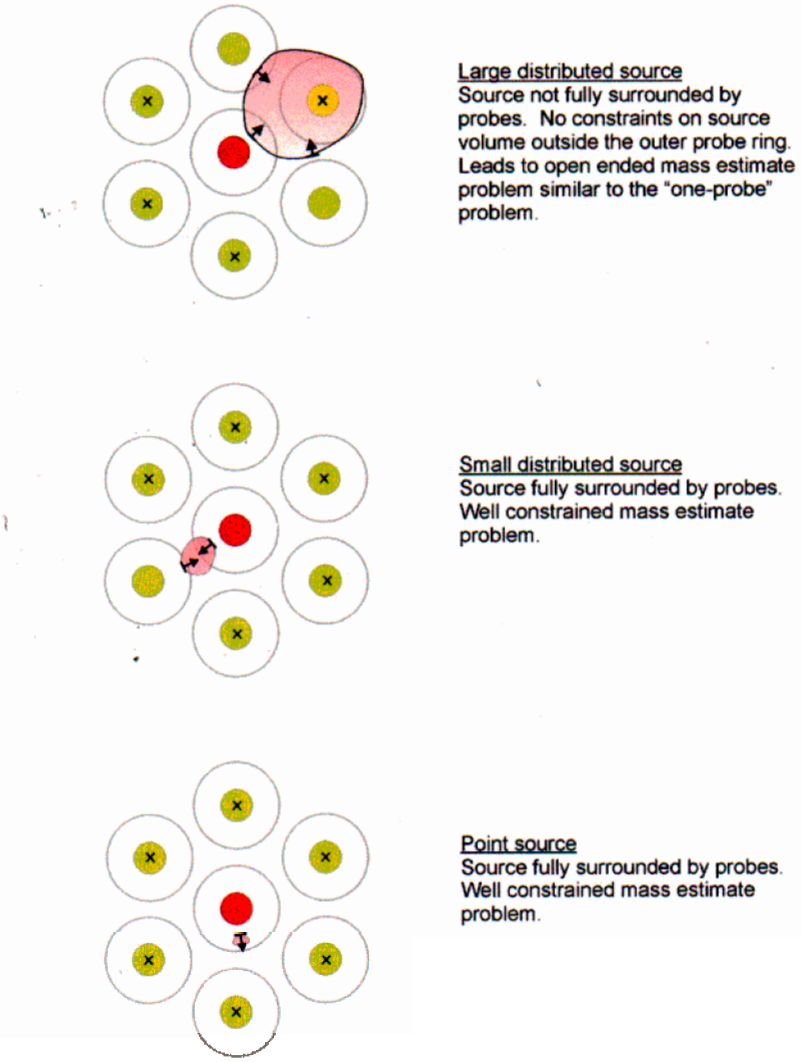

Figure 4-11. Examples of uniform continuous source solutions.

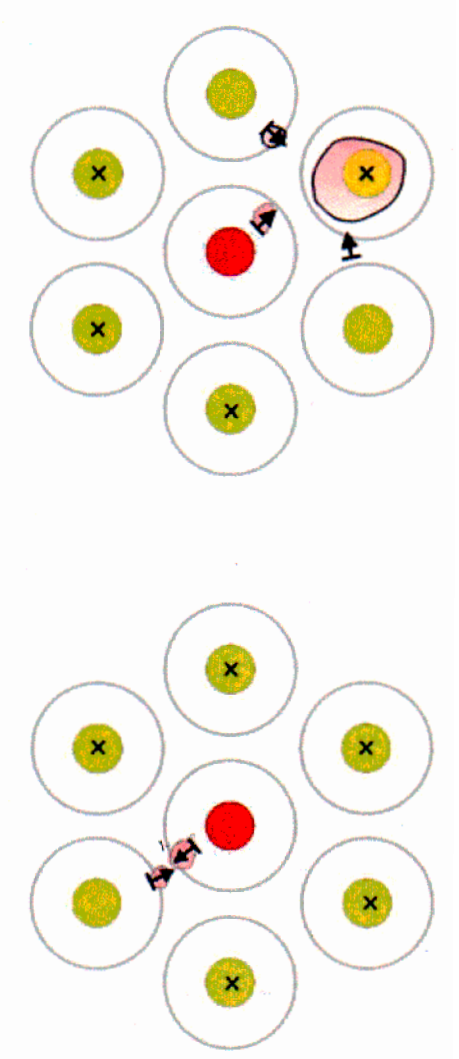

Large distributed source
Alternative solution to scenario 1 that corresponds to a lesser Pu mass. Not sure the two solutions can be easily distinguished.

Small distributed source
Alternative solution to scenario 2 that corresponds to a lesser Pu mass. Not sure the two solutions can be easily distinguished.

Figure 4-12. Examples of alternative point source solutions.

The first thing to note is that a very large source volume extending beyond the outer probe ring creates the same open-ended problem we have seen with P9-20; however, more probes can always be installed to fully constrain the problem.

Once the problem is constrained, i.e. the source is surrounded with probes, and two solutions can be computed: one representing the uniform and continuous case and one representing a series of point sources. Both cases must satisfy all the logging data in all the probes. For the point source case, additional constraints are used to avoid creating unrealistically dense Pu sources. The point source solution will of course give smaller source volume but with higher Pu concentrations. The net result will be a *minimum* Pu mass estimate. The uniform and continuous solution will give a larger source volume with a lower Pu concentration and will be close to *a maximum* Pu mass estimate.

Another possible error source is matrix density. The density is most likely somewhere between 1.6 – 2.0 g/cc (1.8 ± 11%). The density uncertainty is a relatively small factor unless there are some very large voids within the target area.

4.9 Optical Televiewer

Seven visual probes in the SDA were logged with an optical televiewer. The optical televiewer is a digital camera that records 1-mm thick circumferential images from the inside of a visual probe and places or stacks the images as a continuous digital file. The image is spit longitudinally and displayed as a flat image using proprietary software. The resulting picture is analogous to having an image on the inside of a cylinder, cutting the cylinder longitudinally and unrolling or spreading out the image so it can lay flat. The images of the visual probes show tool joints, stabilizers, and the vertical reinforcing bars. The image between the bars is the soil and waste in the landfill taken through the Lexan polymer tubing of the visual probes. Typically, the soil on top of the waste is several feet thick, and the multicolored waste is in the lower sections of the image. The bore hole optical images can be viewed on a share drive, which is called "Hbb2/optical televiewer." To view the images, follow the instructions in the "READ_ME" file, double click on the .exe file, and use file/open when the viewer comes up. The bore hole optical images can also be viewed in Appendix C of this report; however, these images do not reflect the clarity of the originals. Contact Gayle Johnson for original hard copy images in the case file.

5. REFERENCES

Barnes, C. M., 1989, *Evaluation of Cover and Drainage Improvements for Interim Stabilization of the Subsurface Disposal Area at the INEL RWMC*, EDF-BWP-SC-03, Idaho National Engineering Laboratory, EG&G Idaho, Inc., Idaho Falls, Idaho, March 15, 1989.

Beitel, G. A., P. Kuan, C. W. Bishop, and N. E. Josten, 2000, *Evaluation of OU 7-10 Stage I Soil Moisture Readings*, INEEL/EXT-2000-00651, Idaho National Engineering and Environmental Laboratory, Bechtel BWXT Idaho, LLC, Idaho Falls, Idaho.

Borghese, J. V., 1988, *Hydraulic Characteristics of Soil Cover, SDA, INEL: Project Objectives, Sampling, and Determination of Hydraulic Conductivity*, UI-08/88, Thesis under University of Idaho Geology and Geological Engineering Department, Moscow, Idaho, March 1, 1988.

Ebasco Environmental, 1993, *Final EDF (Tasks 23 and 28) SDA Ground Based Geophysics*, Engineering Design File No. ERD-WAG7-14, Idaho National Engineering and Environmental Laboratory, EG&G Idaho, Inc., Idaho Falls, Idaho, March 19, 1993.

GeoSense, 1999, *Surface Geophysical Surveys at INEEL Pit 9 Conducted Under Phase I of the OU 7-10 Contingency Project*, Final Report under Parsons Infrastructure and Technology, Inc., Subcontract No. 734456-T-2821-S002-99, Idaho Falls, Idaho, January 1, 1999.

Griebenow, B. E., 1992, *Technology Evaluation Report for the Buried Waste Robotics Program Subsurface Mapping Project*, EG&G Informal Report No. EGG-WTD-9923, Idaho National Engineering and Environmental Laboratory, EG&G Idaho, Inc., Idaho Falls, Idaho, January 1, 1992.

Hasbrouck, J. C., 1989, *Geophysical Surveys at INEL/RWMC Cold Pit, Acid Pit, and Pit 9*, Subcontractor Report under U.S. Department of Energy Subcontract No. DE-Aco7-86ID12584, UNC Geotech, Grand Junction, Colorado, May 1, 1989.

Josten N. E. and J. C. Okeson, 2000, *OU 7-10 Initial Probing Campaign Downhole Logging Results*, INEEL/EXT-2000-00526, EDF-ER-207, Rev. 0, Idaho National Engineering and Environmental Laboratory, Bechtel BWXT Idaho, LLC, Idaho Falls, Idaho, September 22, 2000.

Josten, N. E. and R. Thomas, 2000, *Pit 9 Coordinates*, INEEL/EXT-2000-01107, EDF-ER-221, Rev. 0, Idaho National Engineering and Environmental Laboratory, Bechtel BWXT Idaho, LLC, Idaho Falls, Idaho, November 13, 2000.

Lange, K. P., 1999, *Pit 9 Overburden Soil Depth*, EDF-ER-056, Idaho National Engineering and Environmental Laboratory, Bechtel BWXT Idaho, LLC, Idaho Falls, Idaho, May 10, 1999.

McElroy D. L., 1993, *Soil Moisture Monitoring Results at the Radioactive Waste Management Complex of the Idaho National Engineering Laboratory*, EGG-WM-11066, Idaho National Engineering and Environmental Laboratory, EG&G Idaho, Inc., Idaho Falls, Idaho.

McElroy D. L. and J. M. Hubbell, 1990, *Hydrologic and Physical Properties of Sediments at the Radioactive Waste Management Complex*, EGG-BG-9147, Idaho National Engineering and Environmental Laboratory, EG&G Idaho, Inc., Idaho Falls, Idaho.

Miller, Eric C., Jeffrey A. Sondrup, and Nicholas E. Josten, 2002, *Durability and Performance of Grouted Waste Monoliths in the SDA (Draft)*, INEEL/EXT-02-00233, Rev. A, Idaho National Engineering and Environmental Laboratory, Bechtel BWXT Idaho, LLC, Idaho Falls, Idaho, November 7, 2002.

Miller, Eric C. and Mark D. Varvel, 2001, *Reconstructing Past Disposal of 743 Series Waste in the Subsurface Disposal Area for Operable Unit 7-08, Organic Contamination in the Vadose Zone*, INEEL/EXT-01-00034, Rev. 0, Idaho National Engineering and Environmental Laboratory, Bechtel BWXT Idaho, LLC, Idaho Falls, Idaho, May 14, 2001.

Okeson, J. C., 2000, *OU 7-10 Stage I Subsurface Exploration and Treatability Studies Report (Draft)*, INEEL/EXT-2000-00403, Rev. A, Idaho National Engineering and Environmental Laboratory, Bechtel BWXT Idaho, LLC, Idaho Falls, Idaho.

Roybal, L. G., G. S. Carpenter, and N. E. Josten, 1992, *A Magnetic Survey of Pit 9 Using the Rapid Geophysical Surveyor*, Engineering Design File No. ERP-BWP-75, Idaho National Engineering and Environmental Laboratory, EG&G Idaho, Inc., Idaho Falls, Idaho, October 14, 1992.

Sage Earth Science, 1999, *Rapid Geophysical Surveyor Technology Validation and Geonics EM-61 Technology Validation*, Final Report under Bechtel BWXT Idaho, LLC, Subcontract, Idaho Falls, Idaho.

Shakofsky, S., 1995, *Changes in Soil Hydraulic Properties Caused by Construction of a Simulated Waste Trench at the Idaho National Engineering Laboratory, Idaho*, DOE/ID-22121, Department of Energy Idaho Operations Office, Idaho Falls, Idaho, March 1995.

Stoller Corporation, 1995, *INEL Pit 9 Geophysical Surveys*, Subcontract Report for Lockheed Environmental Systems and Technologies Co., Pocatello, Idaho, June 20, 1995.

Wright, D. L., D. V. Smith, and J. D. Abraham, 1999, Preliminary Interpretation and Data Report of the VETEM Prototype Survey of Pit 9, Radioactive Waste Management Complex, and Idaho National Engineering and Environmental Laboratory, Idaho, U.S. Geological Survey Draft Report under U.S. Department of Energy Interagency Agreement No. DE-A107-921D13207, Denver, Colorado.

This page is intentionally left blank.